ISSN 1674-1056
http://cpb.iphy.ac.cn
http://iopscience.iop.org/cpb
中国物理 B
Chinese Physics
中国物理 Chinese Physics B

Pressure-induced isostructural phase transition in α-$Ni(OH)_2$ nanowires

Xin Ma(马鑫), Zhi-Hui Li(李志慧), Xiao-Ling Jing(荆晓玲), Hong-Kai Gu(顾宏凯), Hui Tian(田辉), Qing Dong(董青), Peng Wang(王鹏), Ran Liu(刘然), Bo Liu(刘波), Quan-Jun Li(李全军), Zhen Yao(姚震), Bing-Bing Liu(刘冰冰)

Citation: Chin. Phys. B . 2019, 28(6): 066402. **doi:** 10.1088/1674-1056/28/6/066402
Journal homepage: http://cpb.iphy.ac.cn; http://iopscience.iop.org/cpb

What follows is a list of articles you may be interested in

Variational and diffusion Monte Carlo simulations of a hydrogen molecular ion in a spherical box

Xuehui Xiao(肖学会), Kuo Bao(包括), Youchun Wang(王友春), Hui Xie(谢慧), Defang Duan(段德芳), Fubo Tian(田夫波), Tian Cui(崔田)

Chin. Phys. B . 2019, 28(5): 056401. **doi:** 10.1088/1674-1056/28/5/056401

Equation of state of $LiCoO_2$ under 30 GPa pressure

Yong-Qing Hu(户永清), Lun Xiong(熊伦), Xing-Quan Liu(刘兴泉), Hong-Yuan Zhao(赵红远), Guang-Tao Liu(刘广涛), Li-Gang Bai(白利刚), Wei-Ran Cui(崔巍然), Yu Gong(宫宇), Xiao-Dong Li(李晓东)

Chin. Phys. B . 2019, 28(1): 016402. **doi:** 10.1088/1674-1056/28/1/016402

The effect of dislocations on the thermodynamic properties of Ta single crystal under high pressure by molecular dynamics simulation

Yalin Li(李亚林), Jun Cai(蔡军), Dan Mo(莫丹), Yandong Wang(王沿东)

Chin. Phys. B . 2018, 27(8): 086401. **doi:** 10.1088/1674-1056/27/8/086401

Transport properties of mixing conduction in CaF_2 nanocrystals under high pressure

Ting-Jing Hu(胡廷静), Xiao-Yan Cui(崔晓岩), Jing-Shu Wang(王婧姝), Jun-Kai Zhang(张俊凯), Xue-Fei Li(李雪飞), Jing-Hai Yang(杨景海), Chun-Xiao Gao(高春晓)

Chin. Phys. B . 2018, 27(1): 016401. **doi:** 10.1088/1674-1056/27/1/016401

Anomalous behavior and phase transformation of α -GaOOH nanocrystals under static compression

Zhao Zhang(张钊), Hang Cui(崔航), Da-Peng Yang(杨大鹏), Jian Zhang(张剑), Shun-Xi Tang(汤顺熙), Si Wu(吴思), Qi-Liang Cui(崔啟良)

Chin. Phys. B . 2017, 26(10): 106402. **doi:** 10.1088/1674-1056/26/10/106402

Pressure-induced isostructural phase transition in α-Ni(OH)$_2$ nanowires*

Xin Ma(马鑫), Zhi-Hui Li(李志慧), Xiao-Ling Jing(荆晓玲), Hong-Kai Gu(顾宏凯), Hui Tian(田辉), Qing Dong(董青), Peng Wang(王鹏), Ran Liu(刘然), Bo Liu(刘波), Quan-Jun Li(李全军)†, Zhen Yao(姚震)‡, and Bing-Bing Liu(刘冰冰)

State Key Laboratory of Superhard Materials, College of Physics, Jilin University, Changchun 130012, *China*

(Received 30 January 2019; revised manuscript received 12 March 2019; published online 8 May 2019)

High pressure structural phase transition of monoclinic paraotwayite type α-Ni(OH)$_2$ nanowires with a diameter of 15 nm–20 nm and a length of several micrometers were studied by synchrotron x-ray diffraction (XRD) and Raman spectra. It is found that the α-Ni(OH)$_2$ nanowires experience an isostructural phase transition associated with the amorphization of the H-sublattice of hydroxide in the interlayer spaces of the two-dimensional crystal structure at 6.3 GPa–9.3 GPa. We suggest that the isostructural phase transition can be attributed to the amorphization of the H-sublattice. The bulk moduli for the low pressure phase and the high pressure phase are 41.2 (4.2) GPa and 94.4 (5.6) GPa, respectively. Both the pressure-induced isostructural phase transition and the amorphization of the H-sublattice in the α-Ni(OH)$_2$ nanowires are reversible upon decompression. Our results show that the foreign anions intercalated between the α-Ni(OH)$_2$ layers play important roles in their structural phase transition.

Keywords: nickel hydroxide, high pressure, synchrotron radiation, isostructural phase transition

PACS: 64.70.Nd, 91.60.Gf, 07.35.+k, 61.05.cp **DOI:** 10.1088/1674-1056/28/6/066402

1. Introduction

Because of its distinctive structures and physical properties, nickel hydroxide has many practical applications in the fields of physics, chemistry, and engineering. These applications include batteries,[1] photocatalysis,[2] electrocatalysis,[3] supercapacitors,[4,5] electrochromic devices,[6,7] electrochemical sensors,[8,9] and so on. Two different crystallographic polymorphs of known nickel hydroxide have been found, which are represented as α- and β-Ni(OH)$_2$.[10] The β-phase nickel hydroxide is present in the natural mineral theophrastite and is isostructural with the triangular-symmetric brucite[Mg(OH)$_2$], and consists of closely packed two-dimensional (2D) Ni(OH)$_2$ principle layer without water or any anions between its layers.[11] The α-phase nickel hydroxide is composed of hydroxyl-deficient β-Ni(OH)$_2$ layers, parallel to the crystallographic *ab* plane intercalated by water molecules and foreign anions.[10] The inserted water molecules and foreign anions have no fixed position but have some freedoms to rotate and translate in the *ab* plane. The α-phase nickel hydroxide is represented by the general formula Ni(OH)$_{2-x}$ $(A^{n-})x/n \cdot y$H$_2$O, where $x = 0.2$–0.4, $y = 0.6$–1, and $A =$ chloride, sulfate, nitrate, carbonate, or other anions.[12] Usually, the hydrated water molecules inherent in the material are omitted from the written formula, and the material is represented by α-Ni(OH)$_2$.

In geophysics and geochemistry, high-pressure studies of hydrous minerals may provide valuable information about the understanding of various geophysical phenomena and found more complex hydrous minerals abundantly in the earth's mantle.[13–15] Among these hydrous minerals, highly symmetry brucite-type hydroxides [M(OH)$_2$, $M =$ Mg, Ca, Ni, Co, *etc.*] have been widely investigated as the simplest prototypes under high pressure. Although these compounds have a layered CdI$_2$ structure in the trigonal space group $P\bar{3}m1$[16] at the ambient conditions, they exhibit different behaviors at high pressure. Pressure-induced reversible amorphization of the entire crystal structure of Ca(OH)$_2$ has been reported at 12 GPa.[17,18] Compared with Ca(OH)$_2$, its isomorphous Mg(OH)$_2$ remains stable and does not amorphize up to 34 GPa.[17,19] The anomalies of Raman and infrared spectra were observed in Co(OH)$_2$ at 11 GPa, which are attributed to hydrogen sublattice amorphization.[20] Subsequent neutron powder diffraction studies of the Co(OH)$_2$ showed that these observed anomalies in Raman and infrared spectra are the result of structural frustration due to H–H repulsion.[21] In β-Ni(OH)$_2$, no structural phase transition was observed up to 25 GPa.[22]

Compared to these simple models, the inherent hydration and the interlayer anions of α-Ni(OH)$_2$ make its structure more complicated, which is close to the case of natural

*Project supported by the National Key Research and Development Program of China (Grant No. 2018YFA0305900), the National Natural Science Foundation of China (Grant Nos. 11874172, 11374120, 11634004, and 51320105007), and the Fund from Jilin University for Science and Technology Innovative Research Team (Grant No. 2017TD-01).

†Corresponding author. E-mail: liquanjun@jlu.edu.cn

‡Corresponding author. E-mail: yaozhenjlu@163.com

© 2019 Chinese Physical Society and IOP Publishing Ltd

hydrous minerals in the mantle. However, there is no high-pressure research report on the complex α-Ni(OH)$_2$ up to now. In this paper, we performed Raman and XRD studies to investigate the structural phase transition of α-Ni(OH)$_2$ nanowires under high pressure. An isostructural phase transition associated with the amorphization of the H-sublattice of hydroxide in the interlayer spaces of the two-dimensional crystal structure were observed at 6.3 GPa–9.3 GPa. Our results suggest that the isostructural phase transition is related to the amorphization of the H-sublattice. This study provides a reference for understanding the behavior of more complex hydrogen-containing compounds under high pressure.

2. Experimental details

The α-Ni(OH)$_2$ nanowires were synthesized by $NiSO_4$ and NaOH under hydrothermal conditions in a Teflon-lined stainless steel autoclave.[23] The structure of the α-Ni(OH)$_2$ nanowires was characterized by x-ray diffraction (XRD) (Rigaku D/max-2500 x-ray diffractometer with Cu–Kα radiation, $\lambda = 1.5406$ Å). The morphologies of the samples were investigated using a transmission electron microscope (TEM, JEOL JEM-2200FS). Raman spectra were collected using a LabRAM HR Evolution Raman system with a 473-nm laser excitation line. High-pressure synchrotron angle-dispersive XRD measurements were performed at 16-BM-D, beamline of the High Pressure Collaborative Access Team (HPCAT) at the Advanced Photon Source (APS), Argonne National Laboratory, with the incident beam wavelength of 0.3066 Å. Part of the XRD experiments was conducted at 4W2 beamline of Beijing Synchrotron Radiation Facility (BSRF). For all the high-pressure experiments, α-Ni(OH)$_2$ nanowires were loaded in a 150-μm hole (sample chamber) of a preindented stainless steel gasket. Pressure was generated by a symmetric diamond-anvil cell at room temperature. The experiment pressure was calibrated using the ruby fluorescence method. Ar was used as the pressure-transmitting medium for all high pressure measurements.

3. Results and discussion

The XRD pattern of the synthesized product is shown in Fig. 1. The diffraction peaks are in good agreement with the monoclinic phase α-Ni(OH)$_2$ from the standard card JCPDF 41-1424. The lattice parameters $a = 0.798$ nm, $b = 0.294$ nm, $c = 1.361$ nm, and $\beta = 91.1°$ are obtained. The diffraction peaks of α-Ni(OH)$_2$ nanowires are sharp and intense, indicating their highly crystalline nature. In addition, there are no diffraction peaks corresponding to other impurities, which indicates the high quality of the synthesized α-Ni(OH)$_2$ nanowires.

Figure 2 shows the transmission electron microscope (TEM) and the high resolution transmission electron microscope (HRTEM) images of the α-Ni(OH)$_2$ nanowires. We can see that the length of the nanowires is up to several micrometers and the diameter is in the range of 15 nm–20 nm [Figs. 2(a) and 2(b)]. The HRTEM image (Fig. 2(c)) of the α-Ni(OH)$_2$ nanowire clearly shows that the interplanar distances $d = 2.04$ Å, which is consistent with the distance between the (304) lattice planes. The SAED pattern (Fig. 2(d)) of the nanowire in Fig. 2(c) reveals that the nanowire exhibits a single-crystal structure.

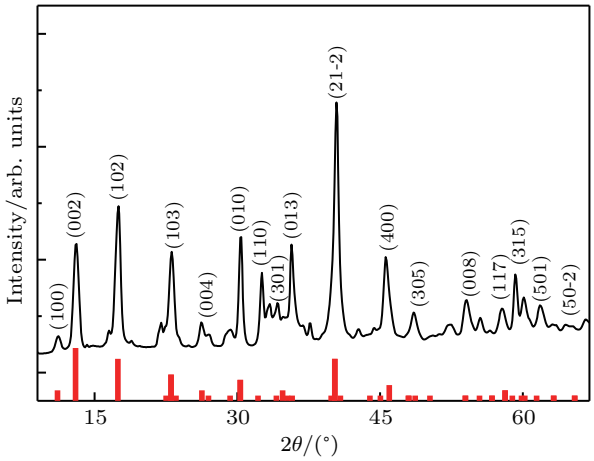


Fig. 1. XRD pattern of α-Ni(OH)$_2$ nanowires. The red bars at the bottom represent the diffraction pattern from JCPDS 41–1424 (wavelength: 1.5406 Å).

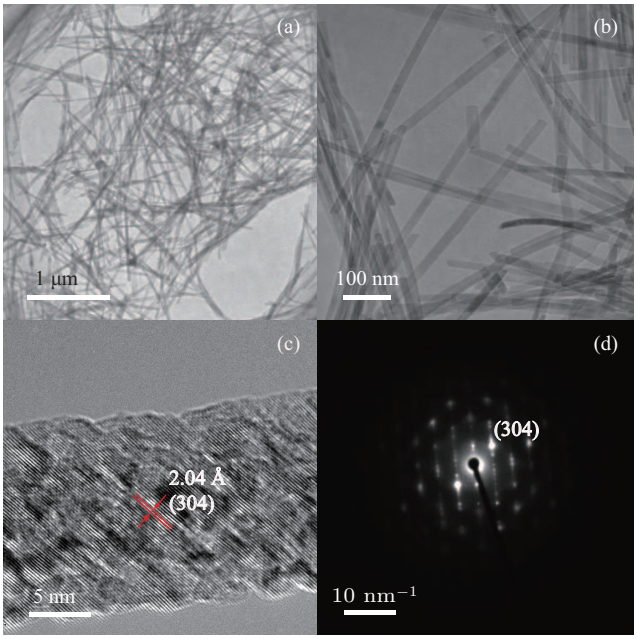


Fig. 2. TEM images [(a) and (b)] and high-resolution TEM (HRTEM) image (c) of α-Ni(OH)$_2$ nanowires, and selected area electron diffraction (SAED) pattern (d) of the single nanowire shown in panel (c).

The selected XRD patterns of α-Ni(OH)$_2$ nanowires under high pressure are shown in Fig. 3. All the peaks of α-Ni(OH)$_2$ shift to smaller d-spacing with increasing pressure, indicating the pressure-induced shrinkage of the unit cells. No

new peaks appear up to the highest pressure of 22 GPa, except the weakening and broadening of these peaks. This suggests that the crystal symmetry does not change obviously. For further detailed analysis, we extract six major strong diffraction peaks from Fig. 3 as a function of pressure change, as shown in Fig. 4(a). From the pressure dependence of the d-spacings, we can observe that two distinct compression regimes can be identified, below 6.3 GPa and above 9.3 GPa. The d-spacing of the selected characteristic peaks decreases with increasing pressure and undergoes a sharp drop above 6.3 GPa. Above 9.3 GPa, the pressure dependence of the d-spacings starts to become flatter than that in the pressure below 6.3 GPa.

The obtained α-Ni(OH)$_2$ nanowires normalized lattice parameters as a function of pressure (Fig. 4(b)) also shows an abnormality in the same pressure range. The pressure dependence of the lattice constants is consistent with the observed variation of d-spacings as a function of pressure. Based on the intercalation chemistry, the presence of foreign ions can increase the thickness of the interlayer space in layered materials. When we apply external pressure to the layered system, the interlayer distance (c axis) reduces significantly more than the intralayer one (a and b axes). This is in accordance with the high pressure behaviors of two-dimensional crystals.[24] Discontinuous changes in a, b, and c axes in the pressure range of 6.3 GPa–9.3 GPa are observed, indicating a structural phase transition occurs. However, there is no obvious crystal symmetry change can be observed from our XRD results. Thus, these results suggest that this phase transition is possibly an isostructural phase transition.

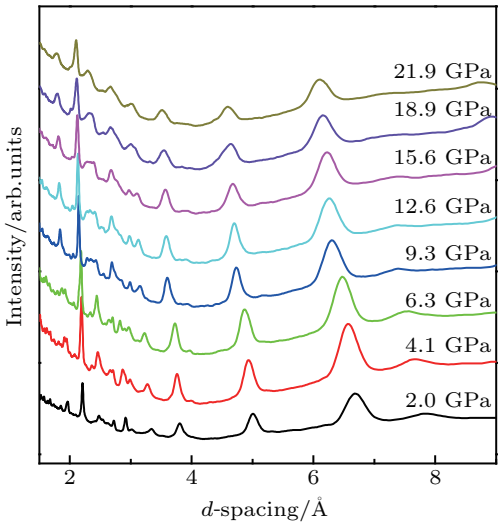


Fig. 3. X-ray diffraction patterns of α-Ni(OH)$_2$ nanowires collected at different pressures.

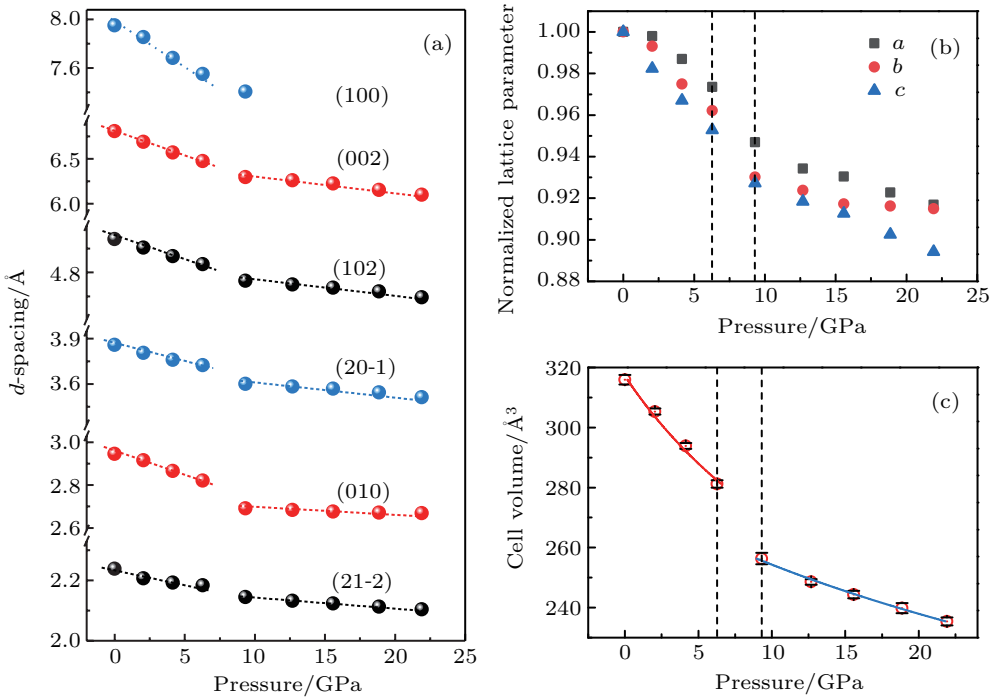


Fig. 4. Structure information of α-Ni(OH)$_2$ nanowires at high pressure. Pressure dependences of the d-spacings (a), normalized lattice constants (b), and unit-cell volume (c) of α-Ni(OH)$_2$ nanowires. The red and blue lines represent the fitting of the low pressure phase and the high pressure phase through the Birch–Murnaghan equation of state, respectively.

As shown in Fig. 4(c), the bulk modulus B_0 of the low pressure phase and high pressure phase are estimated to be 41.2 (4.2) GPa and 94.4 (5.6) GPa, respectively, by fitting the unit-cell volume data with the third-order Birch–Murnaghan equation of state:

$$P = \frac{3B_0}{2}\left[\left(\frac{V}{V_0}\right)^{-7/3} - \left(\frac{V}{V_0}\right)^{-5/3}\right] \times \left\{1 + \frac{3}{4}\left(\mathrm{B}_0' - 4\right)\left[\left(\frac{V}{V_0}\right)^{-2/3} - 1\right]\right\},$$

where P is the pressure, V is the volume at pressure, V_0 is the zero-pressure volume, and B_0' is the derivative of the bulk modulus with respect to pressure (we assumed $B_0' = 4$). The bulk modulus ($B_0 = 41.2$ (4.2) GPa)) of the low pressure phase is much smaller than that of the β-Ni(OH)$_2$ ($B_0 = 88$ GPa, $B_0' = 4.7$),[25] which indicates that α-Ni(OH)$_2$ is more compressible in the initial stage than β-Ni(OH)$_2$. For comparison, the bulk moduli of some hydroxides are shown in Table 1.

Table 1. Comparison of bulk moduli of M(OH)$_2$ compounds

Material	B_0/GPa	B_0'	References
α-Ni(OH)$_2$	phase I 41.2 (4.2) phase II 94.4 (5.6)	4.0 (fixed)	present work
β-Ni(OH)$_2$	88.0	4.7	[22]
Mg(OH)$_2$	54.3 ±1.5	4.7 ±0.2	[38]
β-Co(OH)$_2$	73.3 ±9.5	4.0(Fixed)	[28]
Ca(OH)$_2$	37.8 ± 1.8	5.2 ± 0.7	[16]

The bulk modulus of the low pressure phase of α-Ni(OH)$_2$ is slightly larger than that of Ca(OH)$_2$ but smaller than those of the other hydroxides. The bulk modulus of the high pressure phase of α-Ni(OH)$_2$ is close to that of β-Ni(OH)$_2$ but is much higher than that of the low pressure phase. This indicates that the structure becomes denser and less compressible after the phase transition. In addition, obvious volume collapse is observed during the phase transition (6.3 GPa–9.3 GPa). The observed discontinuous changes of lattice parameters and volume collapse without symmetry change are both the features of the second-order isostructural transformation.[26–28] Therefore, the structural change observed in the α-Ni(OH)$_2$ nanowires can be attributed to an isostructural phase transition.

To further verify the structure phase transition of α-Ni(OH)$_2$ nanowires, we also conducted in situ high-pressure Raman spectra measurements, as shown in Fig. 5. The lattice vibrational modes in Raman spectra of α-Ni(OH)$_2$ nanowires at ambient conditions are observed at 450, 487, and 964 cm^{-1}.[29,30] The two peaks at 987 cm^{-1} and 1081 cm^{-1} in the Raman spectra can be attributed to the SO_4^{-2} vibration.[29] These SO4^{-2} intercalated between the α-Ni(OH)$_2$ layers are foreign anions, which are derived from the reactant NiSO$_4$ during the synthesis process. The internal O–H stretching modes from lattice OH and intersheet H$_2$O are visible from 3520 cm^{-1} to 3650 cm^{-1}.[29] From Figs. 5(b) and 5(c), we can see the pressure dependence of the Raman shifts of α-Ni(OH)$_2$ clearly. As the pressure increases, Raman peaks of lattice modes and SO_4^{-2} exhibit blue shifts (Fig. 5(b)). The characteristic peaks of the lattice modes gradually weaken and disappear above 9.2 GPa, such as those at 450, 487, and 964 cm^{-1}. The vibrational modes of the SO_4^{-2} always exist until the highest pressure in this experiment.

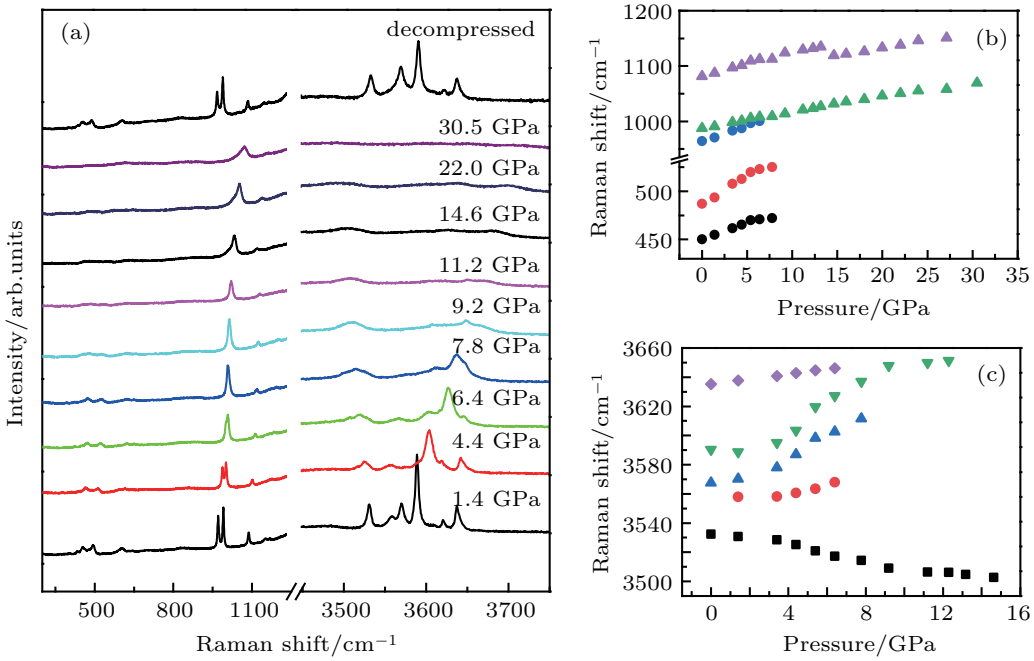


Fig. 5. (a) Raman spectra of α-Ni(OH)$_2$ nanowires at high pressure. (b) Pressure dependence of the Raman shift of the lattice modes and SO_4^{-2} vibration. (c) Pressure dependence of the Raman shift of stretch O–H modes.

From Figs. 5(a) and 5(c), we can observe the vibrational modes of the hydroxyl group in different chemical environments (approx. 3200 cm^{-1}–3700 cm^{-1}). Upon increasing pressure, the Raman peak ($\sim$ 3532 cm^{-1}) of hydroxyl group shows redshift while all other modes exhibit blueshift. The decrease in frequency and broadening of the OH stretching bands of α-Ni(OH)$_2$ with compression. Above 7.8 GPa, the vibrational modes of the hydroxyl group disappear. These results

are consistent with those of brucite-type hydroxides.[17,28,31,32] The brucite structure is characterized by an O–H bond arranged along the *c* axis and surrounded by three cation-oxygen octahedrons in the adjacent layers. Each H atom interacts with three H atoms attached to the neighboring layer. The essence of the strong interaction among H–H and H–O atoms between the neighboring layers of the brucite-type hydroxides at high pressure is still in debate. Most of the recognition is that the broadening and disappear of the OH-stretch modes under high pressure is attributed to the disorder of the O–H bonds, which only involves the disorder of the H-sublattice.[17,19,22,32]

By combining the high pressure XRD and Raman results, we can see that the H sublattice of α-Ni(OH)$_2$ becomes disordered at $\sim$ 7.8 GPa with an isostructural phase transition in the frame structure of α-Ni(OH)$_2$. This result is similar to that of the high pressure study of Co(OH)$_2$ by Nguyen *et al.*[31] Under high pressure, the structure of the brucite-type hydroxides initially compresses primarily along the *c* axis while the cation–oxygen layers remain relatively uncompressed.[33–36] The similar results of α-Ni(OH)$_2$ nanowires lead us to think that it may be similar to the internal structural changes of hydroxide under high pressure. The main interlayer interaction of α-Ni(OH)$_2$ occurs between H–O and H–H of adjacent layers. The change in these interactions under high pressure can be reflected by the OH-stretching modes of α-Ni(OH)$_2$ in Raman spectra. The Raman peaks of hydroxyl group at 3550, 3567, and 3635 cm^{-1} nearly disappear above $\sim$ 7.8 GPa, indicating the pressure-induced amorphization of H sublattice. Obviously, pressure promotes the interaction between the H and O atoms in the adjacent layer leading to the gradual disordering of the H sublattice in α-Ni(OH)$_2$.[37] It is known that XRD is insensitive to the hydrogen position in the crystal lattice. Therefore, the XRD data does not show amorphization characteristics of the H sublattice under high pressure. However, the abrupt slope changes of the lattice parameters varying with pressure are observed at $\sim$ 9 GPa from our XRD results, which indicates α-Ni(OH)$_2$ undergoes an isostructural phase transition.[38–40] This is consistent with the pressure range that observed the amorphization of H sublattice in our Raman results. Based on these results, we suggest that the isostructural phase transition can be attributed to the disorder of the H sublattice. In addition, all the Raman peaks recover when the pressure is released, which shows that the isostructural phase transition and the amorphization of the H sublattice are reversible.

4. Conclusion

In summary, α-Ni(OH)$_2$ nanowires with an average diameter of 15 nm–20 nm and a length of several micrometers were synthesized by hydrothermal method. We investigated the high pressure structural phase transition of the α-Ni(OH)$_2$ nanowires by synchrotron XRD and Raman spectra. An isostructural phase transition takes place at $\sim$ 6.3 GPa–9.3 GPa. Meanwhile, the disorder of the interlayered H-sublattice is observed. Bulk moduli for the low pressure phase and high pressure phase are 41.2 (4.2) GPa and 94.4 (5.6) GPa, respectively. We suggest that the pressure-induced isostructural phase transition in α-Ni(OH)$_2$ nanowires can be attributed to the disorder of the H-sublattice. Both the isostructural phase transition and the amorphization of the H-sublattice in α-Ni(OH)$_2$ nanowires are reversible under high pressure. Our results show that the foreign anions intercalated between the α-Ni(OH)$_2$ layers play important roles in their structural phase transition.

References

[1] Hauel A P 1939 *Trans. Electrochem. Soc.* **76** 435
[2] Ran J G, Yu J G and Jaroniec M 2011 *Green Chem.* **13** 2708
[3] Gao M R, Sheng W C, Zhuang Z B, Fang Q R, Gu S, Jiang J and Yan Y S 2014 *J. Am. Chem. Soc.* **136** 7077
[4] Aghazadeh M, Ghaemi M, Sabour B and Dalvand S 2014 *J. Solid State Electrochem.* **18** 1569
[5] Chen J C, Hsu C T and Hu C C 2014 *J. Power Sources* **253** 205
[6] Mortimer R J, Sialvi M Z, Varley T S and Wilcox G D 2014 *J. Solid State Electrochem.* **18** 3359
[7] Cordoba-Torresi S I, Gabrielli C, Goff A H L and Torresi R 1991 *J. Electrochem. Soc.* **138** 1548
[8] Fan Y, Yang Z J, Cao X H, Liu P F, Chen S and Cao Z 2014 *J. Electrochem. Soc.* **161** B201
[9] Miao Y Q, Ouyang L, Zhou S L, Xu L N, Yang Z Y, Xiao M S and Ouyang R Z 2014 *Biosens. Bioelectron.* **53** 428
[10] Bode H, Dehmelt K and Witte J 1966 *Electrochim. Acta* **11** 1079
[11] McEwen R S 1971 *J. Phys. Chem.* **75** 1782
[12] Yang D N, Wang R M, He M H, Zhang J and Liu Z F 2005 *J. Phys. Chem. B* **109** 7654
[13] Williams Q and Hemley R J 2001 *Ann. Rev. Earth Planet. Sci.* **29** 365
[14] Zhang Z, Cui H, Yang D P, Zhang J, Tang S X, Wu S and Cui Q L 2017 *Chin. Phys. B* **26** 106402
[15] Gao Y P, Dong W Q, Li G and Liu R P 2018 *Chin. Phys. Lett.* **35** 036103
[16] Petch H E and Megaw H D 1954 *J. Opt. Soc. Am.* **44** 744
[17] Kruger M B, Williams Q and Jeanloz R 1989 *J. Chem. Phys.* **91** 5910
[18] Meade C and Jeanloz R 1990 *Geophys. Res. Lett.* **17** 1157
[19] Duffy T S, Meade C, Fei Y W, Mao H K and Hemley R J 1995 *Am. Mineral.* **80** 222
[20] Nguyen J H, Kruger M B and Jeanloz R 1997 *Phys. Rev. Lett.* **78** 1936
[21] Parise J B, Loveday J S, Nelmes R J and Kagi H 1999 *Phys. Rev. Lett.* **83** 328
[22] Murli C, Sharma S M, Kulshreshtha S K and Sikka S K 2001 *Physica B* **307** 111
[23] Dong L H, Chu Y and Sun W D 2008 *Chem. Eur. J.* **14** 5064
[24] Yuan Y F, Zhang Z T, Wang W K, Zhou Y H, Chen X L, An C, Zhang R R, Zhou Y, Gu C C, Li L, Li X J and Yang Z R 2018 *Chin. Phys. B* **27** 066201
[25] Garg N, Karmakar S, Sharma S M, Busseto E and Sikka S K 2004 *Physica B* **349** 245
[26] Efthimiopoulos I, Kemichick J, Zhou X, Khare S V, Ikuta D and Wang Y 2014 *J. Phys. Chem. A* **118** 1713

[27] Manjón F J, Vilaplana R, Gomis O, Pérez-González E, SantamaríaP érez D, Marín-Borrás V, Segura A, González J, Rodríguez-Hernández P, Muñoz A, Drasar C, Kucek V and Muñoz-Sanjosé V 2013 *Phys. Status Solidi B* **250** 669

[28] Pereira A L J, Sans J A, Vilaplana R, Gomis O, Manjón F J, Rodríguez-Hernández P, Muñoz A, Popescu C and Beltrán A 2014 *J. Phys. Chem. C* **118** 23189

[29] Hall D S, Lockwood D J, Poirier S, Bock C and MacDougall B R 2012 *J. Phys. Chem. A* **116** 6771

[30] Cornilsen B C, Karjala P J and Loyselle P L 1988 *J. Power Sources* **22** 351

[31] Nguyen J H, Kruger M B and Jeanloz R 1994 *Phys. Rev. B* **49** 3734

[32] Speziale S, Jeanloz R, Milner A, Pasternak M P and Zaug J M 2005 *Phys. Rev. B* **71** 184106

[33] Nagai T, Hattori T and Yamanaka T 2000 *Am. Mineral.* **85** 760

[34] Parise J B, Leinenweber K, Weidner D J, Tan K and Dreele R B V 1994 *Am. Mineral.* **79** 193

[35] Parise J B, Theroux B, Li R, Loveday J S, Marshall W G and Klotz S 1998 *Phys. Chem. Miner.* **25** 130

[36] Nagai T, Ito T, Hattori T and Yamanaka T 2000 *Phys. Chem. Miner* **27** 462

[37] Shim S H, Rekhi S, Martin M C and Jeanlo R 2006 *Phys. Rev. B* **74** 024107

[38] Wang W D, He D W, Xiao W S, Wang S M and Xu J A 2013 *Chin. Phys. Lett.* **30** 117201

[39] Liu Q Q, Wang F R, Li F Y, Chen L C, Yu R C, Jin C Q, Li Y C and Liu J 2008 *Chin. Phys. Lett.* **25** 2239

[40] Fei Y W and Mao H K 1993 *J. Geophys. Res.* **98** 11875